CHAPTER V
DELIVERY OF CRUDE BONE PROTEIN FORM GELATIN MICROSPHERES AND MICROSPHERES INTEGRATED HYALURONAN-GELATIN BLENDED SCAFFOLD FOR BONE TISSUE REGENERATION

5.1 Abstract

This study aimed to develop a protein delivery HA-Gelatin blended scaffold for bone tissue regeneration. The designed scaffold was composed of gelatin microspheres as the part of integrated delivery device in which the crude bone protein (CBP) extracted from bone extracellular matrix was encapsulated. Gelatin microspheres were prepared with the thermal gelation in water-in-oil emulsion technique. Two types of gelatin (A and B) at three different pH which were physiologic (5.2 and 4.95 for type A and B respectively), 7.4, and 10.0 were specified as the preparative conditions and investigated for their influences on the microspheres properties. The results showed the effect of interaction between gelatin type and pH on microspheres size, zeta potential, swelling ability, and encapsulation of the CBP, but not on the CBP release characteristic. The significantly highest encapsulation of CBP (> 93%) was achieved in gelatin A, pH 10.0 and gelatin B, pH 4.95 microspheres. Astoundingly, the controlled release of CBP from any gelatin microspheres was not observed, implying that the anticipated ionic interaction between CBP and molecules of gelatin may not occur. However, the microspheres integrated composite scaffolds presented phase of sustained CBP release which suggests the essential influence of scaffold matrix on the release mechanism.

(**Key-words**: bone scaffolds; bone protein; gelatin microspheres; controlled release)

5.2 Introduction

Tissue engineering is an approach to regenerate living tissue with an aim at establishing healthy tissue or organ for being a substitute of the damaged or the

diseased tissue (Hoffman, 2002). Progression in tissue engineering research since 1990 has been encouraging a reappraisal of the surgical approach for the treatment of trauma and degeneration of an individual (Hollander and Hatton, 2004). Regarding dental practice, sufficient bone support is a major requirement to achieve favorable function and esthetic in the replacement of a losing tooth with a dental implant. Unfortunately, perfect bone structure is not always presented in most patients. Bone resorption easily occurs even in a simple tooth extraction case as the consequence of would heal process (Jahangiri *et al.*, 1998; Bodic *et al.*, 2005). Prevention of the alveolar bone resorption caused by a tooth extraction has been of great concern, particularly through the principle of tissue engineering (Hanne *et al.*, 1998; Wiesen and Krrzis, 1998; Yaffe *et al.*, 1999; Altundal and Guvener, 2004).

Basically, the fundamental of tissue engineering coalesces cell, supportive material termed "scaffold" and growth-inducing substance to promote three-dimensional tissue growth (Langer and Vacanti, 1993). Scaffold, which is a three-dimensional construct, serves as a temporary territory for cells ingrowths. Ideal scaffold should perfectly imitate the extracellular matrix and provide the necessary support for cells to proliferate and maintain their differentiated function (Hutmacher, 2000; Mikos *et al.*, 2004). Scaffolds design was initially focused on their capabilities in supporting cell growth mostly at the physical and mechanical aspects. However, the design has been recently paradigmatically shifted to serve the function of a cellular guidance. This deliberation is in accordance with the concept of cellular guidance which has been extensively discussed and progressively revised as a new knowledge of the cell-material interaction in tissue regeneration (Causa *et al.*, 2007; Tessmar and Gopferich, 2007). Scaffolds have been designed as a route to transport biological factors for cell growth and differentiation and be able to guide and induce cell adhesion, proliferation, differentiation or even recruit the desired cells. The novel tissue engineering scaffold, therefore, can be considered as a special type of drug delivery apparatus (Tessmar and Gopferich, 2007), or as a drug delivery scaffold.

Drug delivery scaffold can be designed by the integration of a drug encapsulated delivery device into a designated scaffold. Such model has been broadly studied for their efficacy in controlled release and tissue engineering

enhancement (Kimura *et al.*, 2003; Kasper *et al.*, 2005; Holland *et al.*, 2005; Lee and Shin, 2007). The drug delivery device itself has been designed in several profiles and configurations. However, most systems base on the encapsulation or entrapment of active substances in biocompatible polymeric devices (Baldwin and Saltzma, 1998). Among numerous applicable drug delivery devices, Gelatin microspheres have been frequently studied with several therapeutic agents such as antihypertensive (Vandervoort and Ludwig, 2004), signaling proteins like albumin (Lee *et al.*, 2007), chondroitin 6-sulfate (Brown *et al.*, 1998), bFGF (Kimura *et al.*, 2003), IGF and TGF-β (Holland *et al.*, 2005), or even the plasmid DNA (Kasper *et al.*, 2005) can also be encapsulated in gelatin microspheres in which the release profiles was under control. These studies demonstrated satisfactory results of controlled release and tissue regeneration in animal test (Brown *et al.*, 1998). Gelatin microsphere apparently is a utility drug delivery device.

Gelatin is commonly used in pharmaceutical and medical application due to its biocompatibility and biodegradability. Structurally, gelatin is a heterogeneous mixture of single or multiple stranded polypeptides (and their oligomers) each of which contains about 300-4000 amino acids (Tabata and Ikada, 1998; Young *et al.*, 2005; Chaplin, 2007). Molecules of gelatin are polyelectrolyte, presenting diverse isoelectric point (IEP) which are about 3-5 and 7-9 for the alkaline and acidic treated gelatin, respectively. Gelatin with different IEP can be selectively used to from complex with the oppositely charged molecule like proteins, to be the polyion complexation which is quite stable and improbable to dissociate simultaneously. Polyion complexes thus are durable than bonding between low molecular weight electrolytes (Young *et al.*, 2005).

With an aim to regenerate bone in the dental socket, the crude bone protein (CBP) extracted from bone extracellular matrix is the material of interest. CBP evidently encompasses enormous active proteins and growth factors (Somerman *et al.*, 1983; Syftestad and Caplan, 1984; Hauschka *et al.*, 1986; Cho *et al.*, 1992; Hou *et al.*, 2000) which facilitates new bone formation (Urist, 1965; Somerman *et al.*, 1983). Extraction of the crude bone protein with the intricate procedures does not obliterate bioactivities of those factors, and these presumptions initiate the plan to exploit CBP extracted from demineralized bone in regenerating bone tissue by

applying the concept of the polyion complexation in achieving a degree of molecular interaction between gelatin microspheres and CBP.

This contribution proposes to fabricate a novel scaffold used for alveolar bone regeneration. On the basis of multi-functional scaffold, scaffold is designed and expected to function as not only a delivery device of the crude bone protein but also a supporting structure for the growth of bone cells. Concept of the polyion complexation is applied to achieve a degree of ionic-molecular interaction between the gelatin microspheres and crude bone protein. And it is also applied in fabricating a porous scaffold of which the polyelectolyte HA-gelatin blends are the materials of choice. The encapsulated gelatin microspheres are anticipated to be securely bound in the scaffold and provide controlled release of the crude bone protein in order to facilitate bone tissue regeneration.

5.3 Experimental Section

5.3.1 Materials

Gelatin from porcine skin (type A, Bloom no.170-180) was purchased form Fluka (Switzerland). Gelatin form bovine skin (type B, Bloom no.175-225) was purchased from Sigma Aldrich (USA). Hyaluronan (MW 1.35×10^6) was purchased from Coach Industries Inc (Japan). Albumin from bovine serum, tetramethylrhodamine conjugate (MW 66,000 Da) was purchased from Molecular Probes Inc (USA). Rhodamine protein label kit was purchased form Pierce (USA). Saturated Glutaraldehyde aqueous solution (5.6 M) was purchased from Fluka (Switzerland). 1-ethy-3-(3-dimethylaminopropyl)carbodiimide (EDC) was purchased form Fluka (Switzerland). Acetone (AR grade) was purchased from Lab-Scan (Thailand). All other chemical agents were of analytical grade and used without further purification.

5.3.2 Gelatin microspheres preparation

Gelatin microspheres were prepared by a thermal gelation technique with modification. In detail, 10 ml of 15% w/v gelatin (type A or B) aqueous solution was prepared at 40°C. In addition to the physiologic pH which is 5.2 or 4.95 for the gelatin type A or B respectively, pH of the gelatin solution was adjusted to be 7.4

and 10.0 by adding 1N HCl or 1M NaOH with an aim to study the effects of pH and type of gelatin on behaviors of the as-prepared microspheres. Then, the solution was added dropwise into 200 ml of Soya oil preheated at 40°C under continuously stirring at 1,000 rpm with a homogenizer to form water-in-oil emulsion. After 10 min, temperature of the emulsion was reduced to be 4°C with an ice bath while stirring was continued for an additional 30 min to induce physically thermal gelation of the gelatin. Afterward, 200 ml of pre-cooled (4°C) acetone was added and stirred for the next 60 min in order to dehydrate and flocculate the coaceravate droplets. The microspheres were collected by filtration through a sintered glass filter (1 μm pores size) under vacuum, washed three times with 100 ml of cool (4°C) acetone to remove residual oil, and dried in air at room temperature over 24 h.

To crosslink the gelatin microspheres, 250 mg of the dry microspheres was suspended in 10 ml of acetone-water (2:1, v/v) containing 1% (w/v,~100mM) Glutaraldehyde solution and stirred at 4°C, 500 rpm for 1 h. The crosslinked microspheres were collected through a sintered glass filter and washed with precooled (4°C) acetone. Then, the crosslinked microspheres were suspended in 20 ml of 10 mM aqueous glycine solution containing Tween 80 (0.1 wt%), shaken at 37 °C, 50 rpm for 1 h to block the residual aldehyde groups of the unreacted glutaraldehyde. The crosslinked microspheres were then washed twice with 60 ml of the cool deionized water (4°C), with cool acetone, filtered, and eventually air-dried at room temperature for over 24 h.

5.3.3 Crude Bone Protein preparation

CBP was extracted from the bovine jaws bone. In particular, bone was initially washed and cleaned thoroughly in tap water and then sectioned into small pieces with a diamond disc driven by a rotor. Pieces of bones were further crushed into powder in liquid Nitrogen. Then, the as-prepared powder was immersed in 0.6 N HCl at 4°C and shaken continuously on an orbital shaker. After three days, the bony solution was centrifuged and the supernatant was collected, dialyzed for 48 h and lyophilized. The dry CBP was kept in desiccators until use.

5.3.4 Fluorescent labeling of Crude Bone Protein

Crude Bone Protein was fluorescent-labeled with the 5-(and 6)-carboxytetramethylrhodamine, succinimidyl ester (NHS-Rhodamine). Briefly, 10 mg/ml of CBP solution was prepared with 50mM borate buffer, pH 8.5 and transferred to a reaction tube. Then, 10 mg/ml of NHS-Rhodamine in DMSO was added. The reaction solution was gently mixed well and incubated in the dark at room temperature for 1 hour. To remove the non-reacted NHS-Rhodamine, the reaction solution was filtered through a D-salt dextran desalting column using 10 mM phosphate buffered saline (PBS) with 0.15 M NaCl as a filtrating medium. The effluent solution was collected in 500-µl fraction. All fractions were subsequently detected by measuring the absorbance with spectrophotometer at 280 nm to identify the fraction containing NHS-Rhodamine-labeled CBP (hereafter, CBP-Rhod). The concentration of the CBP-Rhod existing in the selected fraction was further determined using spectrofluorometer (Cary Eclipse™) at 541 and 572 nm for the excitation and emission wavelength respectively, based on a BSA-Rhod (Molecular Probes™) standard curve over the concentration range 1-50 µg/ml (r^2=0.996). The CBP-Rhod fraction was stored at 4°C and protected from light until ready to use.

5.3.5 CBP-Rhod loading into gelatin microspheres

Crosslinked gelatin microspheres were loaded with CBP-Rhod by diffusion method. In particular, the aforementioned CBP-Rhod fraction was diluted with 10 mM PBS, 0.15 M NaCl, pH 7.2 to achieve the concentration ~700 µg/ml. Gelatin microspheres were immersed in the diluted CBP-Rhod solution to attain the loading dose of 4 µg CBP-Rhod per mg dried microspheres. The resulting mixture was vortexed for 1 h and incubated at 4°C for 24 h to let the CBP-Rhod infuse. The impregnated microspheres were frozen at -40°C for 24 h, lyophilized, and kept in the dark at 4°C until use.

5.3.6 Fabrication of porous composite hyaluronan-gelatin scaffolds

Porous composite hyaluronan-gelatin scaffolds were fabricated by the solvent casting and freeze-drying technique. Briefly, 2% (w/w) aqueous solution of a HA and gelatin mixture (1:1, w/w) was prepared at 50°C and left to cool down to room temperature. Then, in order to facilitate the blending of HA and gelatin, ionic

strength of the mixture was adjusted by adding the equal amount of NaCl to HA (1:1, mole/equ) and being mixed up for 30 min. The resulting mixture became clearer and more translucent. To crosslink the polymers, calculated amount of EDC (1x to HA, mole/equ) was added and reacted under 200 rpm stirring at room temperature for 2 h. Afterward, the neat or the CBP-Rhod labeled microspheres were suspended in HA-gelatin mixture at 1% (w/w) concentration, which equals to 50% (w/w) of the polymer weight. The suspension was continuously stirred until the microspheres were well dispersed in the mixture and the then was cast in polypropylene discs at a constant weight, freezed at -40°C and lyophilized at -50°C. The samples were kept in desiccators until use.

5.3.7 Characterization

5.3.7.1 Size and morphology of gelatin microspheres and microspheres integrated HA-Gelatin scaffold

Gelatin microspheres were initially inspected under the computer connected Polarizing Optical Microscope (DMRXP, Leica) at 20x magnification. The images were recorded and further used to measure the diameters of the microspheres with the UTHSCSA Image Tool version 3.0 software. One hundred microspheres were measured for each preparative condition and the average values of their sizes were calculated. The data were also used to determine size distribution of the microspheres both before and after crosslinking with 100mM Glutaraldehyde. For the morphological study, gelatin microspheres and the as-prepared scaffolds were mounted on brass stubs, coated with gold using a JEOL JFC-1100 sputtering device, and observed for their microscopic morphology using JEOL JSM-5200 scanning electron microscopy (SEM).

5.3.7.2 Swelling ability of gelatin microsphere

Swelling ability was determined by the alteration of microspheres' size after water uptake. 20 mg of the dry crosslinked microspheres were incubated in 10 ml of 10 mM PBS with 0.15 M NaCl at 37°C for 24 h. Then, sizes of the swelling microspheres were examined with the same procedure as previously described in 5.3.7.1. One hundred microspheres of each preparative

condition were measured and the average diameters were calculated. The swelling ability was calculated according to the following equation:

$$\text{Swelling} = \varnothing_{swell} / \varnothing_{dry}$$

where $\varnothing_{swell}$ and $\varnothing_{dry}$ are the averaged diameter of the microspheres before and after incubation, respectively.

5.3.7.3 Zeta potential determination

Zeta potentials (or electrophoretic mobility) of the gelatin microspheres were determined using Zeta-Meter 3.0+ (Zeta-Meter, Inc., USA). Briefly, the suspension of 25 mg gelatin microspheres in 10 ml of deionized water was filled in an electrophoresis cell. Two electrodes were inserted into the cell and connected to the Zeat-Meter 3.0+ unit. Once the electrodes were energized, microspheres were aroused to move toward one electrode. A microsphere was observed under a microscope for its movement along a specific distance which was indicated by a built in grid. The zeta potential value was detected at a right time point when the microsphere moved to the end. Measurement was repeated 10 times for each preparative condition and the average values were calculated.

5.3.7.4 Actual loading of CBP-Rhod in gelatin microspheres

Five mg of Rhodamine-labeled gelatin microspheres were suspended in 1 ml of 10 mM PBS with 0.15 M NaCl in a 1.5 ml microcentrifuge tube. The tube was then placed in cool water and sonicated with the Sonicator (Vibracell™, Sonic, USA) at 20% amplitude. After 1 h, the suspension was centrifuged at 5,000 rpm for 5 min and the supernatant was collected. The actual amount of the CBP-Rhod in supernatant was determined using spectrofluorometer (Cary Eclipse™) by the same procedure done in the step of NHS-Rhodamine labeling (2.4). The experiment was carried out in triplicate and the results were presented in terms of Encapsulating efficiency of CBP-Rhod (EE) and Loading capacity of gelatin microspheres (LC), which were determined according to the following equation (Freiberg and Zhu, 2004):

$$\text{Encapsulating efficiency (\%)} = \frac{\text{total µg CBP-Rhod encapsulated}}{\text{initial µg CBP-Rhod loaded}} \times 100$$

$$\text{Loading capacity (\%)} = \frac{\text{total mg CBP-Rhod encapsulated}}{\text{total mg microspheres}} \times 100$$

5.3.7.5 In vitro CBP-Rhod release

In vitro release of CBP-Rhod from gelatin microspheres and the microspheres integrated HA-gelatin scaffold were investigated in buffer solution by a standard sampling-separation method. In the release assay, 5 mg of the CBP-loaded microspheres and one piece of the microspheres integrated HA-gelatin scaffold (circular shape with 10 mm in diameter and 2 mm in height), which contained 2.5 mg of gelatin microspheres, were separately immersed in 1 mL of 10 mM PBS with 0.15 M NaCl, and incubated in a shaking water bath (70 rpm) at 37°C. At a given time point, 500 µl of the buffer solution (hereafter, the sample solution) was withdrawn and an equal amount of fresh medium was added in order to maintain a constant volume of the medium. The sample solution was centrifuged at 5000 rpm for 5 min at room temperature and the amount of CBP-Rhod in the sample solution was determined by spectrofluorometry at 541 and 572 nm for the excitation and emission respectively, as previously described. An average value was calculated at each time point. The experiment was done in triplicate.

5.3.8 Statistical analysis

Data were analyzed using the SPSS software version 14.0 for window. Initially, the normal distribution was assessed by the Shapiro-Wilk test. The normal distribution data, representing the homogeneity of the variances, shown by the Levene's test, were then investigated by the one-way analysis of variance (ANOVA) with the Tukey HSD post hoc multiple comparisons. Otherwise, the Dunnett T3 would be applied if the data did not exhibit the homogeneity of the variances. For the data of which the normal distribution was absent but the variance was homogeneous, the Kruskal-Wallis H was applied. To compare the means between 2 data groups, the students' unpaired t-test was used. The significant level was indicated at $p < 0.05$ in any case.

5.4 Results and Discussion

5.4.1 Morphology of gelatin microspheres and microspheres integrated HA Gelatin scaffold

The selected SEM images of the uncrosslinked gelatin microspheres are shown in Figure 5.1. As observed, the microspheres prepared at any given condition presented entirely spherical geometry with a smooth surface, on which the macroscopic pores were not detected. Aggregation of the various sizes microspheres into many small clusters was shown in all cases. In our opinion, such aggregation was caused by the direct contact between the adjacent particles once the solvent was expelled during microspheres preparation. The electrical charge on the surface of particles might be diminished in dry environment so that the electrostatic repulsive force was also weakened; as a consequence, repulsion among particles was unlikely illustrated.

Figure 5.2 show the selected SEM images of internal architecture of the composite HA-gelatin scaffold. A well-defined porous structure and the inter-pore connectivity were observed throughout the bulk. The incorporated gelatin microspheres were extensively embedded into the wall of scaffold without deterioration of their geometry. Nevertheless, exceptional for the quite small particles, almost microspheres were not thoroughly submerged in thin walls of scaffold. This manifestation may be responsible for controlled release of the absorbed protein since the releasing medium could transport through the exposed microspheres differently from the one covered with walls of scaffold.

5.4.2 Effect of gelatin type and pH on size of the gelatin microspheres

Upon the preparation of gelatin microspheres by thermal gelation technique, the average size of particles depends on several manufacturing parameters, for instance, the type and dimension of stirrer, diameter of the vessel or container, volume ratio between aqueous and oil phases and their respective viscosities, stirring speed, and the surface tension between the two immiscible phases governed by type of the selected oil phase (Arshady, 1990). In this study, all parameters were identically controlled in order to investigate the effect of gelatin type and pH on the microspheres size, and it was found that sizes of the as-prepared microspheres varied from ~4 to ~40 μm in which over 85% of the microspheres range between ~8 to ~25 μm (Figure 5.3). For all given conditions, the size distributions presented a similar pattern of which the curves of normal distribution were observed.

The average sizes of the as-prepared gelatin microspheres at various conditions are presented in Figure 5.4. Diameters of the uncrosslinked samples range between ~10 and ~20 μm for gelatin A microspheres, and between ~11 and ~ 23 μm for gelatin B microspheres. Average sizes of the microspheres were apparently in the same dimensional range for any preparative condition. However, when the data were statistically analyzed with the Univariate analysis of variance; test of between-subjects effects, sizes of the as-prepared microspheres were significantly different through the influence of the interaction between type of gelatin and pH. Effect of gelatin type or pH on microspheres size, therefore, can not be individually analyzed. The data were thus reorganized into six discrete groups and analyzed further with one-way ANOVA. The results presented that sizes of both gelatin A and B microspheres prepared at pH 7.4 and 10.0 are statistically the same, in contrast to the microspheres prepared at their physiologic pH at which gelatin A microspheres were significantly smaller than those of gelatin B. The effect of interaction between gelatin type and pH are thus limited at a certain condition, probably only at the physiologic pH.

Considering the crosslinked samples, only gelatin A microspheres prepared at its physiologic pH (pH 5.2) presented a significant reduction in particle size comparing with the others which were ~11 and ~15 μm respectively. The difference in particle sizes might be due to the difference in crosslinking intensity of gelatin A from the others which was particularly favored at its physiologic pH, resulting in a denser network and smaller particle sizes (Vandervoort and Ludwig, 2004). Such observation was also detected in the size of swelling microspheres. Since the CBP was anticipated to be incorporated into gelatin microspheres by diffusion method, swelling ability of the microspheres was required to facilitate absorption of the CBP solution. The as-prepared microspheres illustrated ability to absorb and retain water as the hydrated swelling characteristic was remarkably observed in every study group (Figure 5.5). With the crosslinking condition done in this study, the as-prepared microspheres could swell in water significantly at ~1.3 to 1.6 folds over their sizes in the dry state (Table 5.1). However, the difference of their swelling ability was not noticeably observed at any particular preparative condition.

The type of gelatin used and pH, thus, did not have a clear effect on the resulting size of the microspheres behaving in the uncrosslinked, crosslinked or swelling condition. The result of this study partially corresponded to that of Vandervoort and Ludwig in 2004 which found that type of gelatin did not influence the resulting size of nanoparticle prepared by desolvation method whereas the pH did (Vandervoort and Ludwig, 2004).

5.4.3 Zeta potentials

The zeta potentials value of the microspheres was measured at all given conditions with an aim to study the influence driven from gelatin type and pH. The value would also be beneficial in the study of CBP loading and releasing through gelatin microspheres.

Zeta potentials values of the as-prepared microspheres are shown in Figure 5.6. Evidently, both gelatin A and B microspheres presented different zeta potentials values at different pH. In addition, those samples prepared with the same type of gelatin but at different pH also presented different zeta potentials values. Only the pH 10.0 at which statistic analysis was carried out due to the zeta potential values were so close as ~ -54 and ~ -58 mV for gelatin A and B microspheres, respectively in order to ensure the significance of difference. The analysis revealed their statistically different, therefore, both type of gelatin and pH do have significant influences on the zeta potential value of the microspheres obtained.

Since zeta potential is an indicator of charge density (Brown *et al.*, 1998), the pH-induced disparity of zeta potential value can be explained with the isoelectric point (IEP), which factually is the pH at which net molecular charge and thus zeta potential is equal to zero. The IEP of gelatin A and B are ~9 and ~5, respectively (Vandervoort and Ludwig, 2004; Young *et al.*, 2005), bringing about a different electrical charge of both gelatin types in function of the pH. The electrical charges of gelatin A and B are both positive at their physiologic pH since the pH was under IEP. At pH 7.4, gelatin A has a net positive charge by the under-IEP pH, while gelatin B is charged negatively by the over-IEP pH. And eventually at pH 10.0 which is over the IEP, they both present negative charge.

Concerning gelatin microspheres, the IEP of type A and B gelatin microspheres located somewhere in between pH 7.4-10.0 and pH 4.95-7.4,

respectively (see Figure 5.6). The IEP of the obtained microspheres corresponded to the theoretical IEP of gelatin precursor at any given pH. Therefore, the procedure of microspheres preparation used in this study, the thermal gelation in water-in-oil emulsion technique, does not affect the microspheres zeta potentials.

5.4.4 Loading of CBP in gelatin microspheres

Encapsulation of CBP into gelatin microspheres in this study was on the basis of polyion complexation. It was expected that a degree of molecular interaction was able to take place between bone proteins and gelatin microspheres of opposite charges (Young *et al.*, 2005); as a consequence, a higher yield of the ionic complexes should result in higher encapsulation efficiency and loading capacity (Tabata and Ikada, 1998; Hoffman, 2002; Young *et al.*, 2005).

In order to overcome either the inactivity of bone protein from those procedures of microspheres preparation or the low loading yield of bone protein which was available in limited quantity, this study designed to incorporate CBP into the preformed empty gelatin microspheres by rehydrating the freeze-dried gelatin microspheres with a solution of the CBP-Rhod at 4°C for 24 h. Such condition should be favorable for the complete absorption (Tabata and Ikada, 1998). The amount of CBP-Rhod that had been loaded in gelatin microspheres was reported as either the encapsulating efficiency (EE) or the loading capacity (LC) as shown in Table 5.2.

As observed, the EE of CBP-Rhod ranges highly between ~70 to ~ 90 % for both gelatin types. Comparatively, pH was deemed to influence on the EE with an opposing manner between gelatin A and B microspheres. The EE in groups of gelatin A microspheres was found to be significantly highest at pH 10.0 in which the electrostatic charge was negative; whereas such statistically indifferent highest EE was also found in groups of gelatin B microspheres but at the physiologic pH in which the charge was positive (see also Figure 5.6). Basing on the polyion complexation, this observation suggests the existence of both positively and negatively charged protein molecules in the crude bone extracts.

In addition, the encapsulation of CBP was not only influenced by the pH but also the gelatin type. The EE at pH 10.0 was found to be significantly different between gelatin A and B microspheres while the EE at pH 7.4 were

insignificantly different. A disparity of zeta potential value due to pH change was not the only answer of the case as shown by the Univariate analysis of variance; test of between-subjects effects (data not shown) that the interaction between gelatin type and pH affect significantly to the EE and LC. As a consequence, both factors could not be separately considered.

Concerning the LC, the result ranges between ~ 280 to ~370 µg of the CBP-Rhod per 100 mg of microspheres. Reliance of the LC on type of gelatin and pH at any given condition was found to be identical with the EE. Therefore, the encapsulation of the CBP into microspheres evidently depends on both type of the gelatin and pH.

5.4.5 In vitro CBP-Rhod release

5.4.5.1 CBP-Rhod release form gelatin microspheres

The CBP-Rhod release form gelatin microspheres and the composite scaffolds were presented in term of CBP-Rhod cumulative releasing percentage from which the actual quantity of CBP-Rhod loaded in gelatin microspheres was calculated, as shown in Figure 5.7.

The profiles of CBP-Rhod release form gelatin microspheres are apparently different from the composite scaffolds. Though the release profiles are similar at any given condition of either gelatin microspheres or the composite scaffolds, the amounts of CBP-Rhod release are remarkably different. In particular, the extremely high and low release is observed at the pH 10.0 of gelatin B and A microspheres respectively, where as those of the other conditions are quite the same. However, all profiles astoundingly illustrate the initial burst release of CBP-Rhod within the first hour which was about 73-96 %.

In order to study the CBP release kinetics, the semi-empirical equation based on a power-law expression was introduced as follows (Ritger and Peppas, 1987a; Arifin *et al.*, 2006)

$$Mt/M\infty = kt^n$$

where $Mt/M\infty$ is the fractional release of the CBP-Rhod, k is a constant concerning the structure and geometry of the releasing device and n is the releasing exponent indicating the mechanism of drug release. By using the least

square method, the k and n can be detected from a profile in the plot of log Mt/M∞ as a function of log t (min), as presented in Figure 5.8 and Table 5.3.

From the log Mt/M∞ - log t plot, The CBP-Rhod release profiles showed biphasic modulation characterized by an initial relatively rapid release period within the first 30 minutes followed by a slower release phase. The phase separation is indicated by the difference of the n value calculated as the slope of a straight line fitted to the profile with a satisfactory high correlation coefficient (see table 5.3). The n values of all samples are close to zero particularly in phase 2 which is the slower release phase, leading the factor "t^n" of the semi-empirical equation close to 1 at any time point. Comparatively, the results are much different form what have been theoretically identified as the n values of the monodispersed sphere are 0.43 and 0.85 for Fickian diffusion and the Case-II transport respectively, or 0.30 and 0.45 respectively for the mixture of multiple sizes microspheres (Ritger and Peppas, 1987a, b). The CBP-Rhod releases from gelatin microspheres, therefore, are constant and hardly depend on the time observed. The fast release implies that the anticipated polyion complexation between the CBP-Rhod and gelatin microspheres did not completely occur. This may be due to the molecule of Rhodamine which from the covalent amide bond to primary amine on the protein restricts the ionic interaction between the molecules of protein and gelatin.

5.4.5.2 CBP-Rhod release form composite scaffolds.

Comparing to the gelatin microspheres, the releases of CBP-Rhod from the composite scaffolds are slower and a period of sustained release is illustrated at any preparative condition. The amount of CBP-Rhod release within the first hour was approximately 36-50%. Interestingly, the extremely high and low release is also observed at scaffolds incorporated with pH 10.0 gelatin B and A microspheres respectively.

From the log Mt/M∞ - log t plot, The CBP-Rhod release profiles showed three phases of release according to the calculated n values (see Figure 5.8 and Table 5.3). Phase 1 correlated to an initial burst release of CBP-Rhod from the scaffolds within the first 30 min. The n values in this phase range from 0.37 to 0.62 which correlate to the theoretical value as mention earlier. Phase 2

corresponded to the sustained release of CBP-Rhod starting from 1 hour to 7 days. The n values of this slow release phase are much lesser than those in phase 1, but are in the same range as the n values of the initial burst CBP-Rhod release form gelatin microspheres. Phase 3, eventually, represented the CBP-Rhod release with an increasing rate from phase 2 but not faster than phase 1.

Considering the mechanism of CBP-Rhod release from the composite scaffolds, the initial burst release may be the combination of diffusion and dissolution release since the n values are in between 0.30 and 0.45 (Ritger and Peppas, 1987a, b) (except for gelatin B pH 7.4). Such observation is not found in case of CBP-Rhod release from gelatin microspheres. It is believed that CBP-Rhod might partially release into the HA-Gelatin blended solution in which the CBP-Rhod encapsulated gelatin microspheres were dispersed during the process of composite scaffolds fabrication. As a consequence, the releasing CBP-Rhod was also integrated in the mass of HA-Gelatin scaffolds. The initial burst release, therefore, may be the release from the scaffold matrix instead of the incorporated gelatin microspheres.

The mechanism of the sustained release in phase 2 may be the same as that of the initial burst release form gelatin microspheres, but occurs at a slower rate due to their comparable n values and lesser constant (k) values in most samples of the former case. This observation suggests that the sustained release concerns the release of CBP-Rhod from the incorporated gelatin microspheres exposing into porosities within scaffolds.

During phase 3 release, the degradation of HA-Gelatin scaffold might occur, as being observed during sampling, and induce the exposure of the underneath scaffold matrix including the gelatin microspheres which were previously submerged. The rate of CBP-Rhod release is thus higher, but the mechanism can not be truly described regarding the theoretical n values because the mostly n values of phase 3 are lesser than the lower range of the theoretical n values. However, it is believed that phase 3 release is influenced by degradation and diffusive processes.

In this study, the difference in size between the gelatin microspheres was probably not large enough to result in a significantly different CBP-Rhod release rate (Berkland *et al.*, 2002; Arifin *et al.*, 2006). However, the

ongoing mechanism of the CBP controlled release can be the organization of a diffusion-erosion process contributed by the capability of water uptake into the gelatin microspheres and the ability of protein transportation through the scaffold. Microspheres formulation mainly controls the induction time necessary to achieve protein release while the composition of polymeric scaffold controls the release rate (Ungaro *et al.*, 2006). Therefore, a temporal and spatial control of signaling molecules may be obtained by the combination of the appropriated microspheres and scaffold formulations.

5.5 Conclusion

Type of gelatin and the preparative pH are the two factors that should be considerably controlled in the design of bone protein delivery scaffold which contains gelatin microspheres as an incorporated delivery device. Interaction between those two factors influences significantly on size of the as-prepared microspheres, surface charge or the zeta potential, swelling ability and encapsulation capability of the CBP. This effect, however, is not observed in the drug release studies. The ionic interaction between molecules of bone protein and gelatin in the microspheres was not large enough to provide sustained release of the CBP. Incorporation of the CBP loaded gelatin microspheres into HA-Gelatin blended scaffold create a complex environment and the synergistic functions between gelatin microspheres and scaffold in which controlled release was evidently presented.

5.6 Acknowledgements

The authors acknowledged partial support received from (a) the National Center of Excellence for Petroleum, Petrochemicals, and Advanced Materials (NCE-PPAM), and (b) the Petroleum and Petrochemical College (PPC), Chulalongkorn University.

5.7 References

Altundal, H. and Guvener, O. (2004) The effect of alendronate on resorption of the alveolar bone following tooth extraction. International Journal of Oral and Maxillofacial Surgery, 33(3), 286-293.

Arifin, D.Y., Lee, L.Y., and Wang, C.-H. (2006) Mathematical modeling and simulation of drug release from microspheres: Implications to drug delivery systems. Advanced Drug Delivery Reviews, 58(12-13), 1274-1325.

Arshady, R. (1990) Albumin microspheres andmicrocapsules: methodology of manufacturing techniques. Journal of Controlled Release, 14(2), 111-131.

Baldwin, S.P. and Saltzma, W.M. (1998) Materials for protein delivery in tissue engineering. Advanced Drug Delivery Reviews, 33(1), 71-86.

Berkland, C., King, M., Cox, A., Kim, K., and Pack, D.W. (2002) Precise control of PLG microsphere size provides enhanced control of drug release rate. Journal of Controlled Release, 82(1), 137-147.

Bodic, F., Hamel, L., Lerouxel, E., Basle, M.F., and Chappard, D. (2005) Bone loss and teeth. Joint Bone Spine, 72(3), 215-221.

Brown, K.E., Leong, K., Huang, C.-H., Dalal, R., Dalal, R., Green, G.D., Haimes, H.B., Jimenez, P.A., and Bathon, J. (1998) Gelatin/chondroitin 6-sulfate microspheres for the delivery of therapeutic proteins to the joint. Arthritis & Rheumatism, 41(12), 2185-2195.

Causa, F., Netti, P.A., and Ambrosio, L. (2007) A multi-functional scaffold for tissue regeneration: The need to engineer a tissue analogue. Biomaterials, 28(34), 5093-5099.

Chaplin, M. "Gelatin." Water structure and science 25 June 2008. 24 September 2008 <http://www.lsbu.ac.uk/water/hygel.html>

Cho, M.I., Matsuda, N., Lin, W.L., Moshier, A., and Ramakrishnan, P.R. (1992) In vitro formation of mineralized nodules by periodontal ligament cells form the rat. Calcified Tissue International, 50(55), 459-467.

Freiberg, S. and Zhu, X.X. (2004) Polymer microspheres for controlled drug release. International Journal of Pharmaceutics, 282(1-2), 1-18.

Hanne, E., Sonis, S., Gallagher, G., and Adwood, D. (1998) Preservation of alveolar ridge with hydroxyapatite-collagen implants in rats. The Journal of Prosthetic Dentistry, 60(6), 729-734.

Hauschka, P.V., Mavrakos, A.E., Iafrati, M.D., and Doleman, S.E. (1986) Growth factors in bone matrix, isolation of multiple types by affinity chromatography on heparin-sepharose. Journal of Biological Chemistry, 261(27), 12665-12674.

Hoffman, A.S. (2002) Hydrogels for biomedical applications. Advanced Drug Delivery Reviews, 54(1), 3-12.

Holland, T.A., Tabata, Y., and Mikos, A.G. (2005) Dual growth factor delivery from degradable oligo(poly(ethylene glycol)fumurated) hydrogel scaffolds for cartilage tissue engineering. Journal of Controlled Release, 101(1-3), 111-125.

Hollander, A.P. and Hatton, P.V. (2004). Biopolymer Methods in Tissue Engineering. Totowa, New Jersey: Humana Press.

Hou, L.T., Liu, C.M., Wong, Y., and Chen, J.K. (2000) Biological effects of cementum and bone extracts on human periodontal fibroblasts. Journal of Periodontalogy, 71(7), 1100-1109.

Hutmacher, D.W. (2000) Scaffolds in tissue engineering bone and cartilage. Biomaterials, 21(24), 2529-2543.

Jahangiri, L., Devlin, H., Ting, K., and Nishimura, I. (1998) Current perspectives in residual ridge remodeling and its clinical implications: A review. J Prosthet Dent, 80(2), 244-237.

Kasper, F.K., Kushibiki, T., Kimura, Y., Mikos, A.G., and Tabata, Y. (2005) In vivo release of plasmid DNA from composites of oligo(poly(ethylene glycol)fumurated) and cationized gelatin microspheres. Journal of Controlled Release, 107(3), 547-561.

Kimura, Y., Ozeki, M., Inamoto, T., and Tabata, Y. (2003) Adipose tissue engineering based on human preadipocytes combined with gelatin microspheres containing basic fibroblast growth factor. Biomaterials, 24(14), 2513-2521.

Langer, R. and Vacanti, J.P. (1993) Tissue engineering. Science, 260(5110), 920-926.

Lee, M., Chen, T.T., Iruela-Arispe, M.L., Wu, B.M., and Dunn, J.C.Y. (2007) Modulation of protein delivery from modular polymer scaffolds. Biomaterials, 28(10), 1862-1870.

Lee, S.H. and Shin, H. (2007) Matrices and scaffolds for delivery of bioactive molecules in bone and cartilage tissue engineering. Advanced Drug Delivery Reviews, 59(4-5), 339-359.

Mikos, A.G., Lu, L., Temenoff, J.S., and Tessmar, J.K. 2004. Synthetic bioresorbable polymer scaffolds. In J. E. Lemons (Ed.), Biomaterials science: An introduction to materials in medicine, 2 ed., Vol. 1: 735-749. California: Elsevier Inc.

Ritger, P.L. and Peppas, N.A. (1987a) A simple equation for description of solute release I. Fickian and Non-Fickian release from non-swellable deviecs in the form of slabs, spheres, cylinders or discs. Journal of Controlled Release, 5(1), 23-36.

Ritger, P.L. and Peppas, N.A. (1987b) A simple equation for description of solute release II. Fickian and anomalous release from swellable devices. Journal of Controlled Release, 5(1), 37-42.

Somerman, M., Hewitt, A.T., Varner, H.H., Schiffmann, E., Termine, J., and Reddi, A.H. (1983) Identification of a bone matrix-derived chemotactic factor. Calcified Tissue International, 35(1), 481-485.

Syftestad, T.G. and Caplan, A.I. (1984) A fraction from extracts of demineralized adult bone stimulated the converison of mesenchymal cells into chondrocytes. Developmental Biology, 104(2), 348-356.

Tabata, Y. and Ikada, Y. (1998) Protein release from gelatin matrices. Advanced Drug Delivery Reviews, 31(3), 287-301.

Tessmar, J.K. and Gopferich, A.M. (2007) Matrices and scaffolds for protein delivery in tissue engineering. Advanced Drug Delivery Reviews, 59(4-5), 274-291.

Ungaro, F., Biondi, M., d'Angelo, I., Indolfi, L., Quaglia, F., Netti, P.A., and Rotonda, M.I.L. (2006) Microshpere-integrated collagen scaffolds for tissue engineering: Effect of microsphere formulation and scaffold properties on protein release kinetics. Journal of Controlled Release, 113(2), 128-136.

Urist, M.R. (1965) Bone: formation by autoinduction. Science, 150(3698), 893-899.

Vandervoort, J. and Ludwig, A. (2004) Preparation and evaluation of drug-loaded gelatin nanoparticles for topical ophthalmic use. European Journal of Pharmaceutics and Biopharmaceutics, 57(2), 251-261.

Wiesen, M. and Krrzis, R. (1998) Preservation of the alveolar ridge at implant sides. Periodontal Clinical Investigations, 20(2), 17-20.

Yaffe, A., Binderman, I., Breuer, E., Pinto, T., and Golomb, G. (1999) Disposition of alendronate folllowing local delivery in a rat jaw. Journal of Periodontology, 70(8), 893-895.

Young, S., Wong, M., Tabata, Y., and Mikos, A.G. (2005) Gelatin as a delivery vehicle for the controlled release of bioactive molecules. Journal of Controlled Release, 109(1-3), 256-274.

Table 5.1 Swelling ratio of the gelatin microspheres prepared with gelatin types A (a) and type B (b) at various pH

Type	Condition	Swelling ratio
Gelatin A	pH 5.2 (physiologic)	1.600
	pH 7.4	1.606
	pH 10.0	1.485
Gelatin B	pH 4.95 (physiologic)	1.429
	pH 7.4	1.285
	pH 10.0	1.441

Table 5.2 Encapsulating efficiency of the CBP and Loading capacity of the gelatin microspheres. [a,b,c,d] are significantly different at $p < 0.05$; One-Way ANOVA with Tukey HSD (Mean ± SD, n=3)

Type	Condition	Encapsulating Efficiency (%) ($\mu g_{CBP\ encap}/\mu g_{loaded\ CBP}$)	Loading Capacity (%) ($mg_{detected\ CBP}/mg_{spheres}$)
Gelatin A	pH 5.2	$72.89 \pm 0.12^{a,b}$	$0.291 \pm 0.000^{a,b}$
	pH 7.4	$79.82 \pm 2.33^{b,c}$	$0.319 \pm 0.009^{b,c}$
	pH 10.0	95.90 ± 4.12^{d}	0.383 ± 0.016^{d}
Gelatin B	pH 4.95	92.87 ± 2.22^{d}	0.371 ± 0.009^{d}
	pH 7.4	83.47 ± 2.50^{c}	0.333 ± 0.010^{c}
	pH 10.0	70.48 ± 3.84^{a}	0.281 ± 0.015^{a}

Table 5.3 Constant (k), releasing exponent (n) and correlation coefficient (r^2) of CBP release from gelatin microspheres and microspheres integrated HA-Gel scaffolds at three releasing intervals (n1,n2, and n3). k and n values were calculated with the least squares method.

	Release time					
	0-30 mins			1h-4days		
	k1	n1	r^2	k2	n2	r^2
Gelatin microspheres						
Gelatin A, pH 5.4	0.724	0.003	0.933	0.783	0.012	0.947
Gelatin A, pH 7.4	0.768	0.035	0.977	0.841	0.013	0.952
Gelatin A, pH 10.0	0.598	0.061	0.993	0.701	0.013	0.969
Gelatin B, pH 4.95	0.116	0.043	0.936	0.770	0.008	0.969
Gelatin B, pH 7.4	0.702	0.059	0.974	0.859	0.007	0.970
Gelatin B, pH 10.0	0.879	0.023	0.988	0.912	0.014	0.940

	Release time								
	0-30 mins			1h-7days			8-14 days		
	k1	n1	r^2	k2	n2	r^2	k3	n3	r^2
Composite HA-Gel scaffolds									
Gelatin A, pH 5.4	0.112	0.372	0.960	0.304	0.067	0.993	0.025	0.366	0.971
Gelatin A, pH 7.4	0.073	0.444	0.986	0.271	0.073	0.999	0.032	0.325	0.995
Gelatin A, pH 10.0	0.074	0.426	0.973	0.245	0.069	0.994	0.098	0.180	0.983
Gelatin B, pH 4.95	0.093	0.384	0.982	0.297	0.060	0.996	0.060	0.221	0.993
Gelatin B, pH 7.4	0.050	0.620	0.988	0.337	0.069	0.987	0.064	0.229	0.987
Gelatin B, pH 10.0	0.129	0.384	0.988	0.338	0.070	0.995	0.108	0.180	0.969

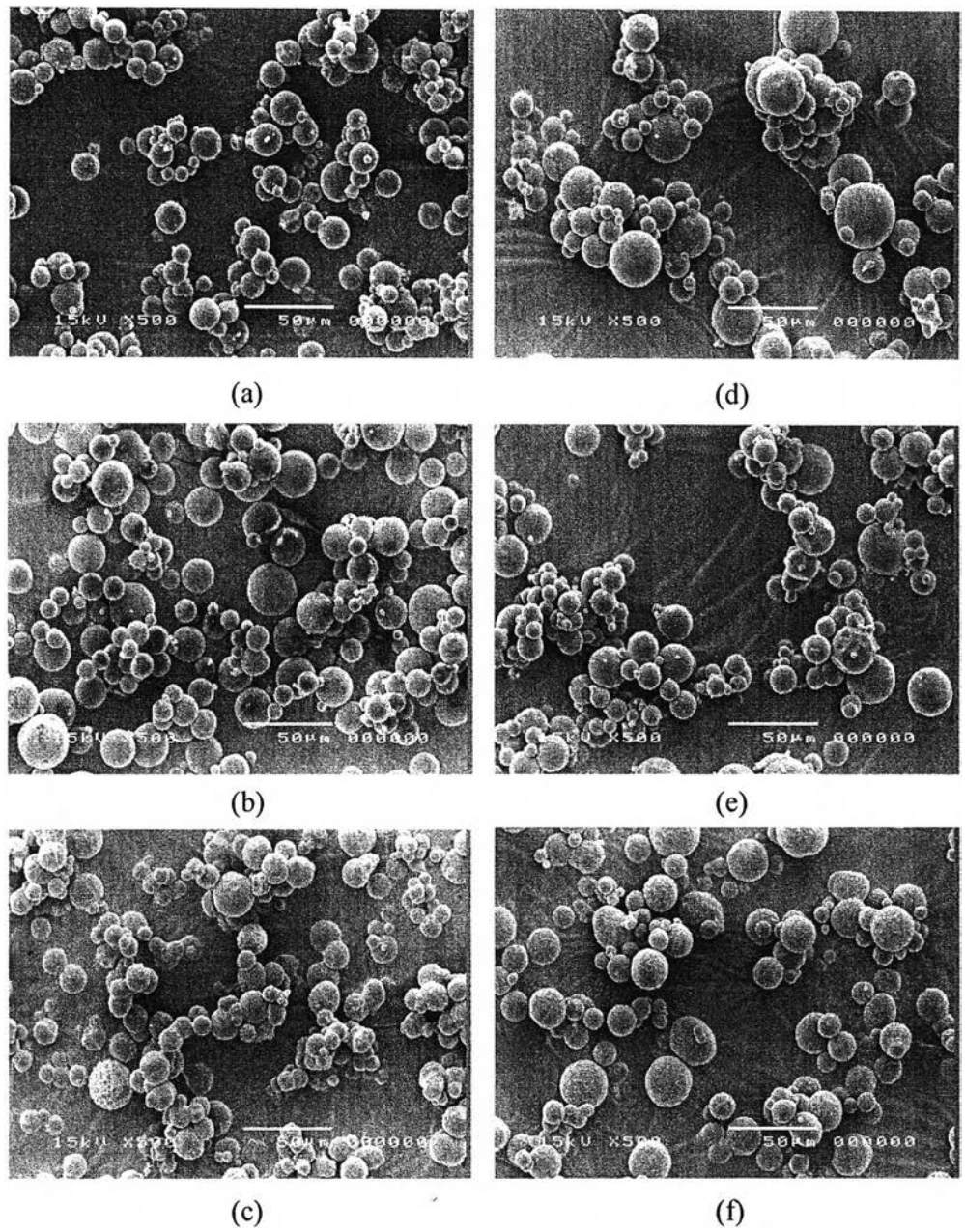

Figure 5.1 SEM images illustrating morphology of the gelatin microspheres prepared with gelatin type A at physiologic pH (5.2) (a), pH 7.4 (b), pH 10.0 (c) and gelatin type B at physiologic pH (4.95) (d), pH 7.4 (e), and pH 10.0 (f).

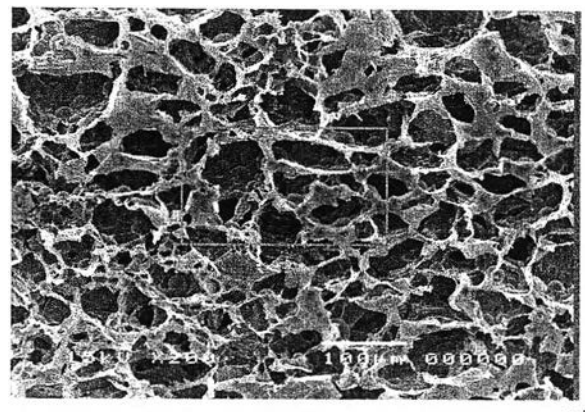

(a)

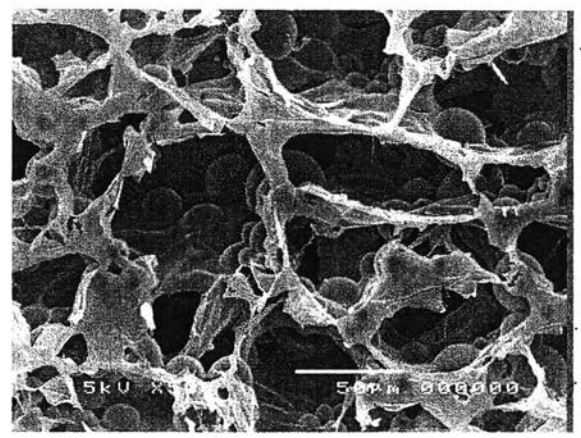

(b)

Figure 5.2 SEM images of the as-prepared microspheres integrated HA-gelatin scaffold illustrate thorough distribution of gelatin microspheres within the scaffold (a) and the embedded gelatin microspheres in the walls of scaffold's chamber (b), (b) is the magnified image of the selected area from (a).

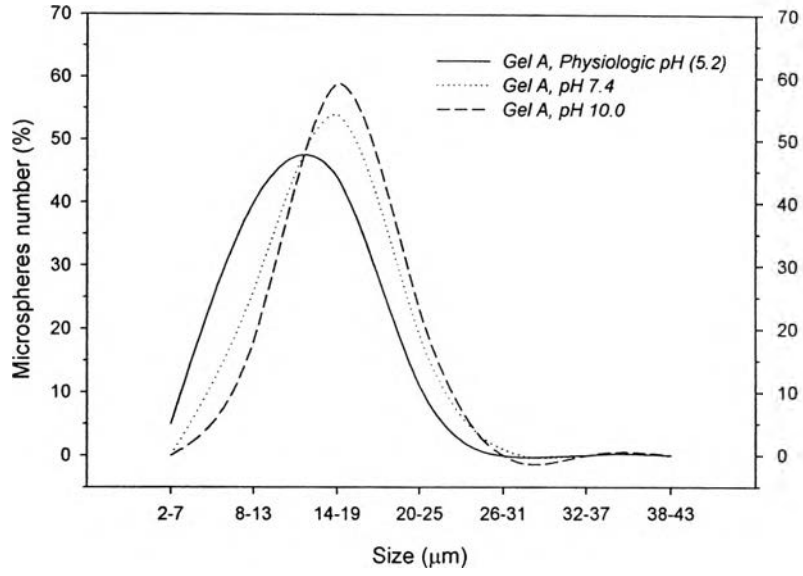

(a)

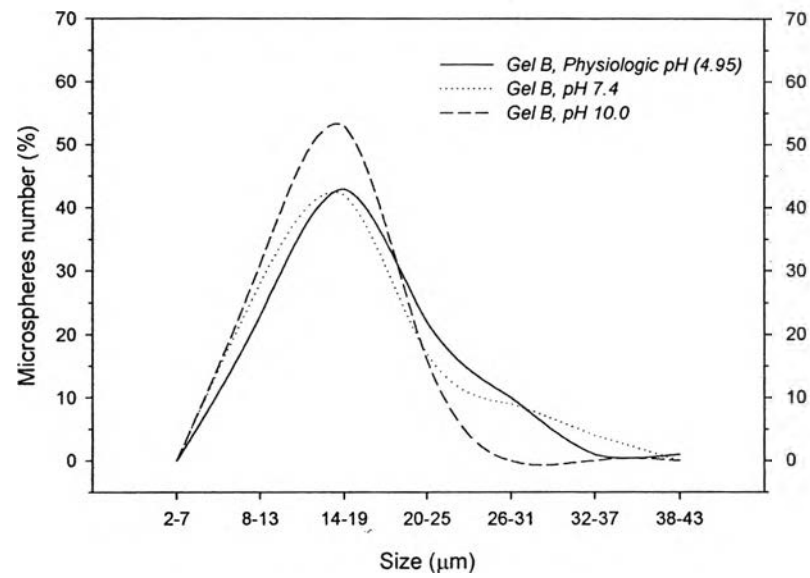

(b)

Figure 5.3 Size distribution of the gelatin microspheres prepared with gelatin types A (a) and type B (b) at various pH (n = 100).

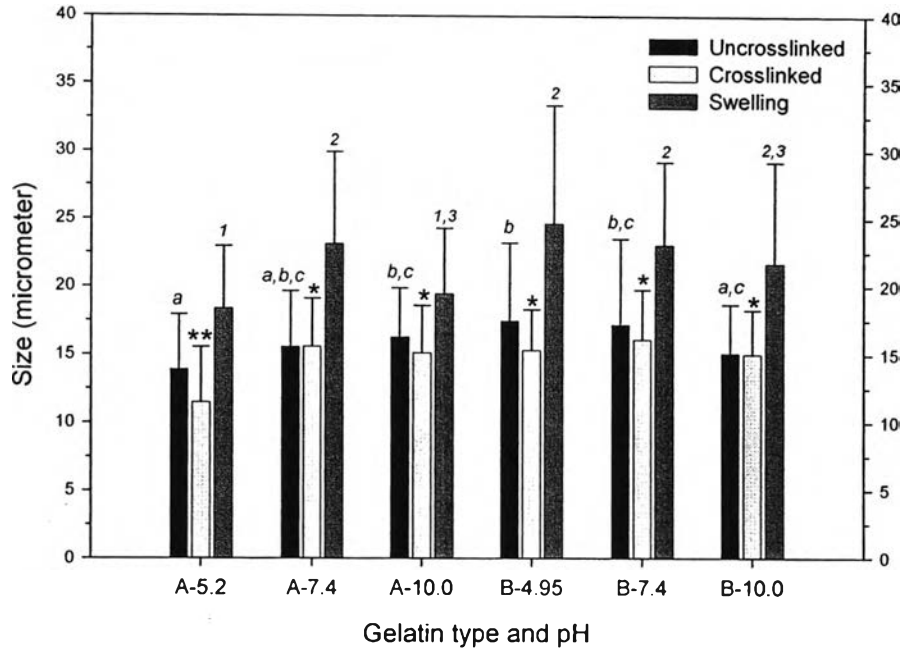

Figure 5.4 Particle sizes of the gelatin microspheres prepared with gelatin types A (a) and type B (b) at various pH and conditions (n = 100). a,b,c, *, 1,2,3 are significantly different at $p < 0.05$; One-Way ANOVA with Dunnett T3.

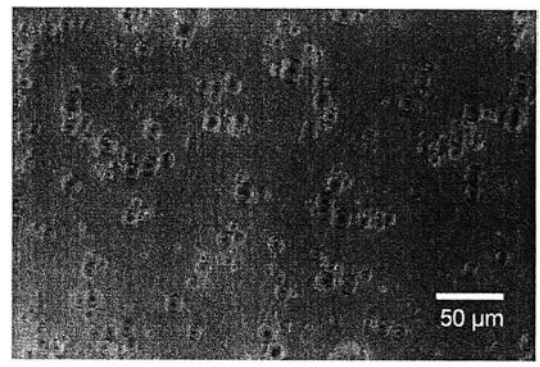

(a)

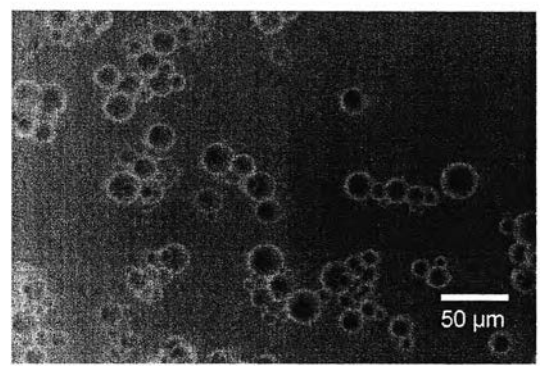

(b)

Figure 5.5 Images from Optical microscope illustrate morphology of uncrosslinked, dry gelatin microspheres (a) and crosslinked, wet and swelling gelatin microspheres (the samples were prepared with gelatin type A at pH 5.2).

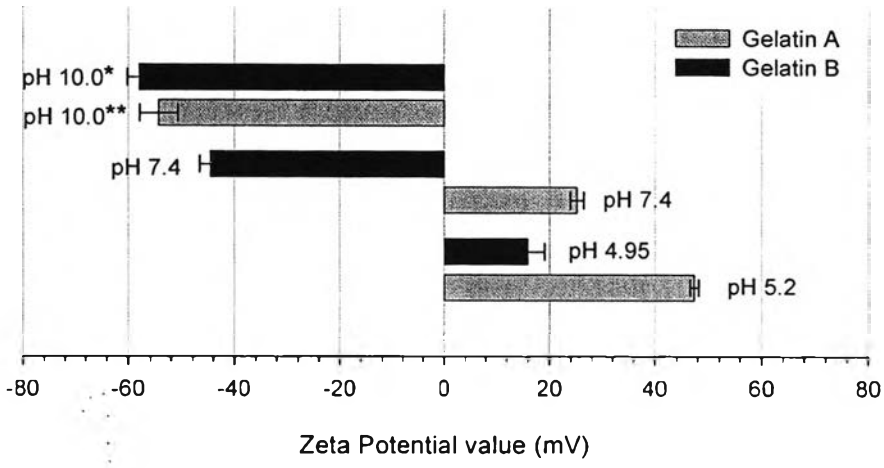

Figure 5.6 Zeta potential values of the gelatin microspheres prepared with gelatin types A and B at various pH. * is significantly different at $p < 0.05$; Students' unpaired t-test.

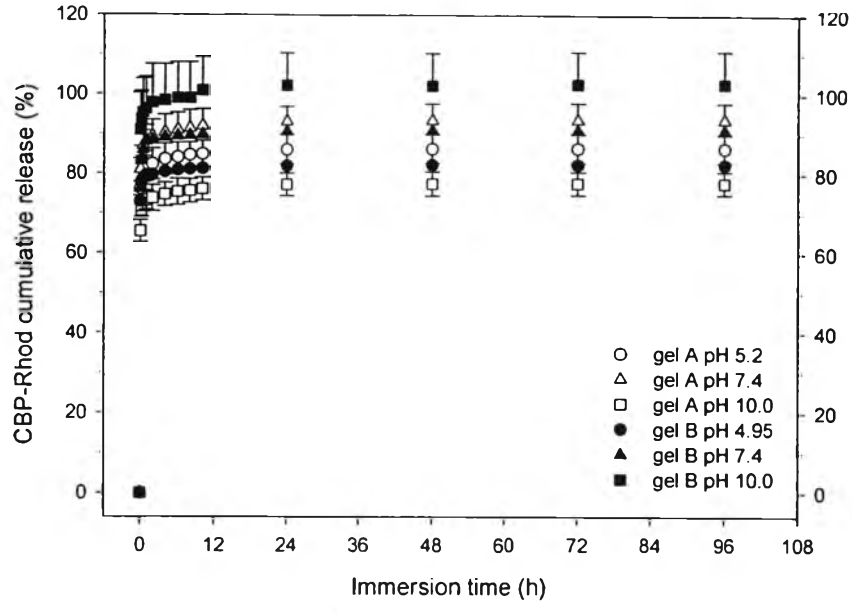

(a)

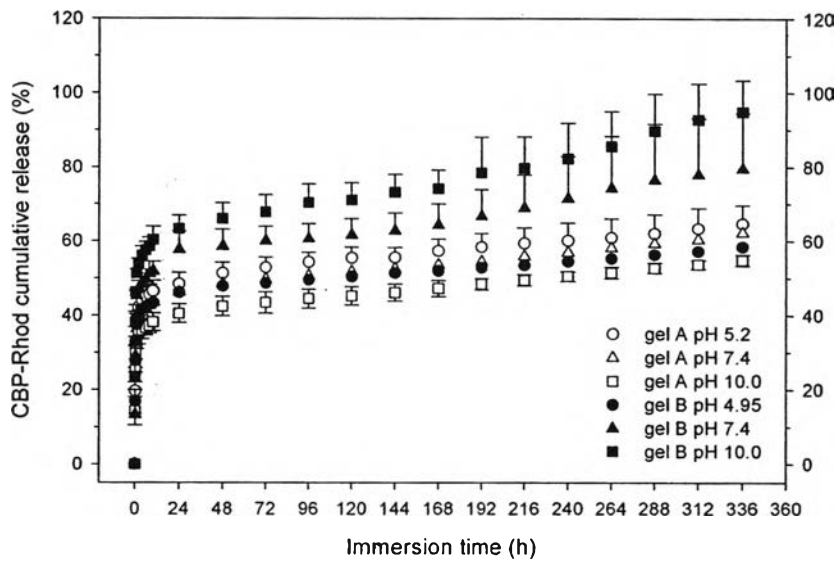

(b)

Figure 5.7 CBP cumulative release (%) from gelatin microspheres (a) and microspheres integrated HA-Gel scaffolds (b).

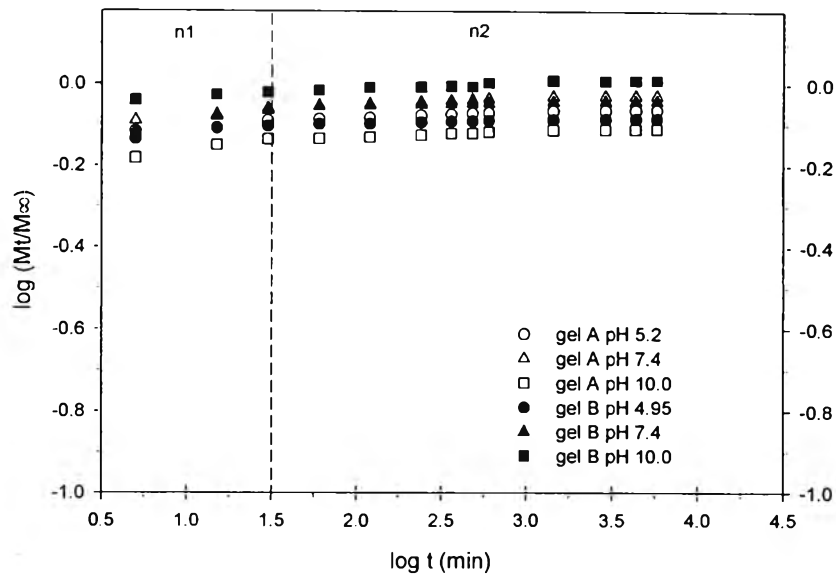

(a)

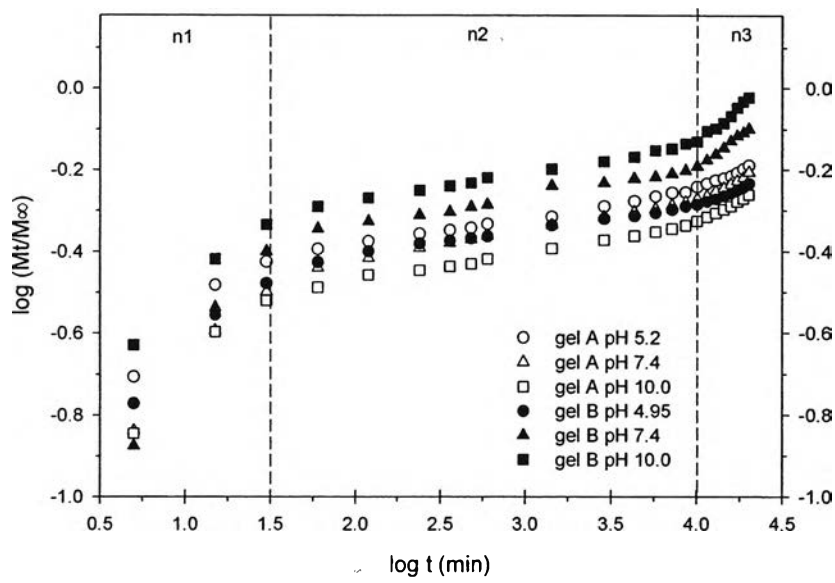

(b)

Figure 5.8 Log Mt/M∞ plotted as a function of log t (min) for CBP release from gelatin microspheres (a) and microspheres integrated HA-Gel scaffolds (b) at three releasing intervals (n1, n2, and n3).